INCLUSIVE AND ISOLATED PHOTONS IN DOUBLE-POMERON-EXCHANGE PROCESSES*

A.K. Kohara, C. Marquet

Instituto de Física, Universidade Federal do Rio de Janeiro
C.P. 68528, Rio de Janeiro 21945-970, RJ, Brazil
and
Centre de Physique Théorique, École Polytechnique, CNRS
Université Paris-Saclay, 91128 Palaiseau, France

(Received November 12, 2015)

We compute prompt photon production in double-Pomeron exchange events in pp collisions at 13 TeV using the resolved-Pomeron-model assumptions. We make use of the proton diffractive pdf imposing specific kinematical constraints from the LHC experiments. For the hard-scattering matrix element computation, we make use of the JetPhox program. We show that NLO contributions must be taken into account in order to constraint quarks and gluons inside Pomeron.

DOI:10.5506/APhysPolBSupp.8.827
PACS numbers: 12.38.Aw, 13.85.Qk

1. Introduction

A large effort has been devoted to understand the QCD dynamics of hard diffractive events in hadronic collisions, since such processes were first observed at HERA [1, 2] and at Tevatron [3, 4] more than 20 years ago.

In deep inelastic scattering (DIS), the HERA Collaboration [5–7] measured the proton structure function $F_2(x, Q^2)$ with good accuracy, however they had found that about 10% of the DIS events are diffractive, which provides a diffractive structure function $F_2^D(\beta, Q^2, \xi, t)$ for the proton, where ξ is the momentum fraction of the proton carried by the Pomeron and $\beta = x/\xi$ is the momentum fraction of the Pomeron carried by the parton emerging from it.

To obtain the proton structure function in DIS, it is well-know that collinear factorization is valid which permits to separate the parton distribution functions (pdf) of the proton and the short-range cross section

* Presented at EDS Blois 2015: The 16$^{\text{th}}$ Conference on Elastic and Diffractive Scattering, Borgo, Corsica, France, June 29–July 4, 2015.

calculated order-by-order in perturbative QCD. It has been proven in [8] that this factorization still holds in DDIS. In order to describe the Pomeron structure function in terms of partons, it is necessary to assume Regge factorization by defining a Pomeron flux and convolute it with the Pomeron's pdfs $f_{i/\mathbb{P}}(\beta, Q^2)$

$$f^D_{i/p}\left(\xi, t, \beta, Q^2\right) = f_{\mathbb{P}/p}(\xi, t) * f_{i/\mathbb{P}}\left(\beta, Q^2\right) . \tag{1}$$

Together, these two types of factorization are ingredients of the resolved Pomeron model (RPM) [9] and have been used at HERA [10] to extract the Pomeron's pdfs.

In spite of successful application of the assumptions above in DDIS, there is an evidence [11] that in hard diffractive hadronic collisions, collinear factorization does not apply. This is possibly explained by the existence of secondary soft interactions that could fill up the rapidity gaps. Nevertheless, this soft interaction should occur on time scales much longer than the hard interactions. In this sense, it is reasonable to keep factorization and absorb the effect of secondary particles in an overall factor called survival probability factor S_{DPE}. With an extension of RPM assumptions to hadron–hadron collisions, the diffractive differential cross section is

$$d\sigma^{pp\to p\gamma Xp} = \mathcal{S}_{\mathrm{DPE}} \sum_{i,j} \int f^D_{i/p}\left(\xi_1, t_1, \beta_1, \mu^2\right) f^D_{j/p}\left(\xi_2, t_2, \beta_2, \mu^2\right) \otimes d\hat{\sigma}^{ij\to\gamma X} , \tag{2}$$

where $d\hat{\sigma}$ is the short-distance partonic cross section computed order-by-order in the perturbation theory (provided the transverse momentum of the photon is sufficiently large). The proton's dpdfs, $f^D_{i/p}$, are non-perturbative objects, however their evolution with the factorization scale μ is obtained perturbatively using the DGLAP [12] evolution equations.

One way to constrain quarks and gluons inside the Pomeron is to measure prompt photons in diffractive proton–proton ($p+p$) collisions, as was suggested in [13]. However, this study relied on leading-order matrix-elements, since the Forward Physics Monte Carlo generator [14] was used. Subsequent works also relied on LO matrix elements [15]. In this proceeding, we want to investigate the effects of higher-order corrections and their impact for a center-of-mass energy of 13 TeV at the LHC, and we shall use instead the JetPhox Monte Carlo [16] to compute the matrix elements at leading order (LO) and at next-to-leading order (NLO).

On the theoretical side, prompt photons refer to high-p_{t} photons created in a hard process, either directly (direct photons) or through the fragmentation of a hard parton (fragmentation photons) [17]. On the experimental side, inclusive and isolated photons denote prompt photons measured without or with an isolation cut, respectively. These are two observables that we shall estimate for double-Pomeron-exchange (DPE) events, meaning diffractive $p+p$ collisions from which both protons escape intact, taking into account the kinematical constraints of the forward proton detectors of the CMS–TOTEM collaborations, or those to be installed by the ATLAS Collaboration in the future [18].

2. Effective diffractive pdfs with experimental constraints

In the following, we assume the intact protons in DPE events to be tagged in the forward proton detectors of the CMS–TOTEM collaborations, or those to be installed by the ATLAS Collaboration in the future [18], called AFP detectors. The idea is to measure scattered protons at very small angles at the interaction point and to use the LHC magnets as a spectrometer to detect and measure them. We use the following acceptances [19]:

— $0.015 < \xi < 0.15$ for ATLAS-AFP,

— $0.0001 < \xi < 0.17$ for TOTEM–CMS.

We denote the diffractive quark and gluon distributions integrated over t and ξ by $q^D(x,\mu^2)$ and $g^D(x,\mu^2)$ respectively. These effective pdfs are obtained from the Pomeron pdfs $q_{\mathbb{P}}(\beta,\mu^2)$ and $g_{\mathbb{P}}(\beta,\mu^2)$, and from the Pomeron flux $f_{\mathbb{P}/p}(\xi,t)$. The latter is integrated over the t variable

$$f_{\mathbb{P}}(\xi) = \int\limits_{t_{\min}}^{t_{\max}} dt\ f_{\mathbb{P}/p}(\xi,t) \qquad \text{with} \qquad f_{\mathbb{P}/p}(\xi,t) = A_{\mathbb{P}} \frac{e^{B_{\mathbb{P}}t}}{\xi^{2\alpha_{\mathbb{P}}(t)-1}}\,. \tag{3}$$

The parameters of Eq. (3) are the slope of the Pomeron flux $B_{\mathbb{P}} = 5.5^{-2.0}_{+0.7}$ GeV^{-2}, and Pomeron Regge trajectory $\alpha_{\mathbb{P}}(t) = \alpha_{\mathbb{P}}(0) + \alpha'_{\mathbb{P}}\ t$ with $\alpha_{\mathbb{P}}(0) = 1.111 \pm 0.007$ and $\alpha'_{\mathbb{P}} = 0.06^{+0.19}_{-0.06}$ GeV^{-2}. The boundaries of the t integration are $t_{\max} = -m_p^2\xi^2/(1-\xi)$ (m_p denotes the proton mass) and $t_{\min} = -1$ GeV^2. The normalization factor $A_{\mathbb{P}}$ chosen such that $\xi \times \int_{t_{\min}}^{t_{\max}} dt\ f_{\mathbb{P}/p}(\xi,t) = 1$ at $\xi = 0.003$.

The constrained dpdf are obtained by the convolution of the integrated Pomeron flux Eq. (3) with the Pomeron pdf in addition to the phase space restrictions over ξ

$$f_{i/p}^D\left(x,\mu^2\right) = \int\limits_{\max(x,\ \xi_{\min})}^{\max(x,\ \xi_{\max})} \frac{d\xi}{\xi}\ f_{\mathbb{P}}(\xi)\ f_{i/\mathbb{P}}\left(x/\xi,\mu^2\right)\,. \tag{4}$$

For the Pomeron pdfs, we make use of the HERA fit B in [10]. These distributions are built in a way to be easily incorporated into the LHAPDF library [20] in the grid format.

3. Computing double-Pomeron-exchange prompt photon production using JetPhox

JetPhox is a Monte Carlo generator built to compute hadronic cross sections for the process $pp \to \gamma X$ using the collinear factorization framework. Cross sections are calculated as a convolution of short-range matrix elements, computed at LO and NLO, and long-range (non-perturbative) parton distribution and fragmentation functions. Therefore, within the resolved Pomeron model (2), this program can also be used to compute the cross sections $pp \to pp\gamma X$ in DPE events. In order to do this, we must substitute the regular pdfs by our effective diffractive pdfs

$$f_{i/p}\left(x,\mu^2\right) \longrightarrow \int d\xi dt d\beta\ \delta(x-\beta\xi)\ f^D_{i/p}\left(\xi,t,\beta,\mu^2\right) \equiv f^D_{i/p}\left(x,\mu^2\right)\ , \quad (5)$$

and multiply the resulting cross sections by the gap survival probability S_{DPE}.

JetPhox produces both inclusive and isolated photons with momentum p_{t} and rapidity y. In the case of inclusive cross section, it sums the direct and the fragmentation contribution in the following way:

$$\frac{d\sigma}{dp_{\mathrm{t}}^2 dy} = \frac{d\hat{\sigma}^\gamma}{dp_{\mathrm{t}}^2 dy} + \sum_a \int dz\ \frac{d\hat{\sigma}^a}{dp_{\mathrm{t}a}^2 dy_a}(p_{\mathrm{t}}/z,y) D_a^\gamma\left(z,\mu^2\right)\ , \quad (6)$$

where $d\hat{\sigma}^a$ is the hard cross section for producing a parton $a=(q,\bar{q},g)$ which will then radiate a high-p_{t} photon during its fragmentation into a hadron. D_a^γ is the fragmentation function, the z variable is $z \equiv p_\gamma/p_a$, and we have chosen the fragmentation scale to be μ. In the case of isolated photons, an additional criteria is imposed on the hadronic activity surrounding the high-p_{t} photon as is discussed later.

In the following, we use JetPhox to compute the direct and the fragmentation contributions in (6), replacing, as explained previously, the regular pdfs by the diffractive pdfs extracted above. Technically, this program calls the pdfs from the LHAPDF library [20]; we replaced one of those parton distribution sets in grid format by our diffractive pdfs constrained with the kinematical cuts. Our choice of factorization scale is $\mu = p_{\mathrm{t}}$.

4. Numerical results

In this section, we detail the future measurements to be performed at the LHC, in order to test the resolved Pomeron model and to constrain the quark and gluon content of the Pomeron, using photon production in DPE processes. We use the Monte Carlo program JetPhox (version 1.3.1) to simulate the results, with 2×10^8 events per channel.

4.1. DPE inclusive photons

In the inclusive mode, there are significant contributions from both direct and fragmentation photons; let us first focus on the direct photons. At LO ($\alpha_{em}\alpha_{\rm s}$), both annihilation processes $q\bar{q} \to g\gamma$, and Compton processes $q(\bar{q})g \to q(\bar{q})\gamma$, contribute. Going to NLO ($\alpha_{em}\alpha_{\rm s}^2$) opens in addition gg-initiated partonic sub-processes, but they contribute only to 1% of the events. In Fig. 1, we analyse the relative contributions between these two channels using ATLAS-AFP acceptance (very similar results are obtained in the TOTEM–CMS case). We observe a large dominance of the Compton scattering over annihilation one. This fact is explained by the dominance of the dpdf of the gluon with respect to the quarks ones at low x.

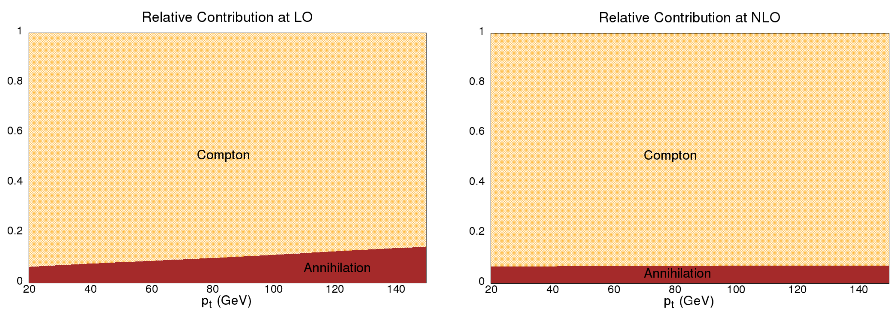

Fig. 1. These figures show, for DPE direct photon production, the relative contributions of the Compton and annihilation processes as a function of photon $p_{\rm t}$. Left: at LO, the Compton process represents about 90% of the differential cross section; the contribution of the annihilation process is slightly increasing with increasing $p_{\rm t}$. Right: at NLO, the Compton process dominates around 95% of the differential cross section for all the $p_{\rm t}$ range analysed.

We display in Fig. 2 (left) the inclusive photon rapidity distribution (for $p_{\rm t} > 20$ GeV) summing all the channels and comparing the results at LO and NLO. We show predictions for both ATLAS-AFP and TOTEM–CMS detectors at 13 TeV, and we note that the difference in magnitude between the LO and NLO calculation is about 20%. In Fig. 2 (right), we show the rapidity distribution over the same conditions as before for the isolated mode as we will explain in the next subsection. Obviously, NLO corrections are not negligible, they must be taken into account in order to extract correctly the Pomeron structure from future data.

Finally, to compare these cross sections with the future data from the experiments, we note that the factor $S_{\rm DPE}$ may have to be readjusted. We have assumed $S_{\rm DPE} \simeq 0.1$, but the actual value is rather uncertain and must first be measured.

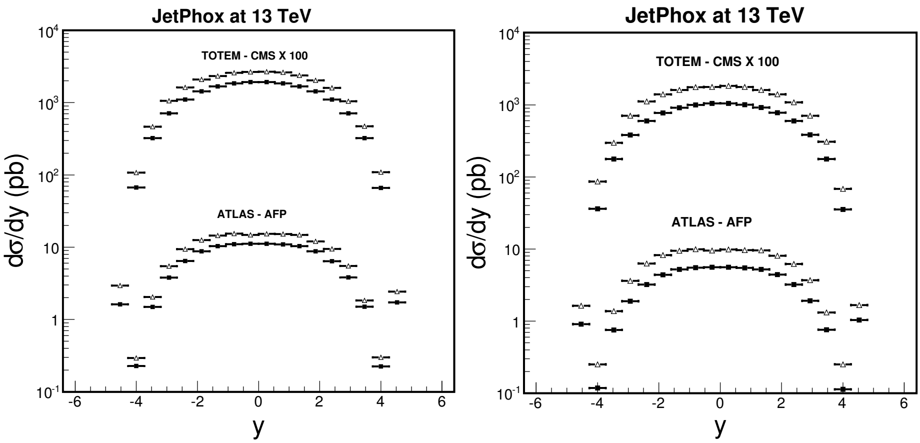

Fig. 2. These figures show the rapidity distributions of DPE inclusive photons (left) ($pp \to pp\gamma X$) and the isolated photons (right) computed by summing the direct and fragmentation contributions for a center-of-mass energy of 13 TeV, for both ATLAS-AFP and TOTEM–CMS detector acceptances. The squares and the triangles represent the LO and NLO calculations, respectively. In the inclusive case, the NLO results give a cross section about 20% greater than the LO results, while in the isolated case this percentage increases to 50%. In both figures the TOTEM–CMS distributions have been multiplied by a factor of 100 to better discriminate them from ATLAS-AFP predictions.

4.2. DPE isolated photons

In order to suppress the contribution from fragmentation processes, one can use an isolation criteria. We require that the hadrons measured within a cone of radius $R = 0.4$ around the photons have a maximum transverse energy of 4 GeV. This is one of the options available in JetPhox [16], we checked that our conclusions are independent of this particular choice.

In Fig. 2 (right), we display our predictions for the rapidity distribution of DPE isolated photons, for both experimental acceptances detectors at 13 TeV. We note that the NLO cross sections are about 50% greater than the LO ones, which is a much bigger difference than in the inclusive case.

The comparison between the inclusive and isolated photon production is also presented in Fig. 3 showing the relative contribution of the direct and the fragmentation processes at NLO. The relative contribution of fragmentation processes is decreasing with increasing p_{t}, but it remains always large in the inclusive case: between 20 and 150 GeV, it goes from 50% to 25%. In the isolated case, however, it is clear that the fragmentation contribution is strongly suppressed by the isolation criteria, and as the transverse momentum of the photon increases, this contribution eventually becomes negligible.

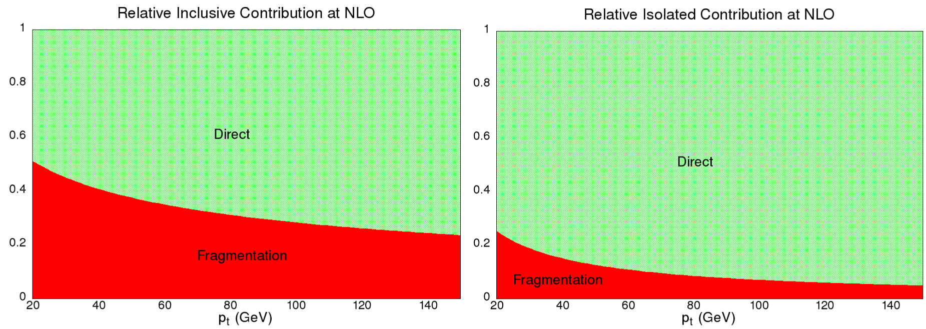

Fig. 3. These figures show, for DPE prompt photon production at NLO, the relative contributions of the direct and fragmentation processes as a function of photon $p_{\rm t}$. Left: in the inclusive case, the direct and fragmentation contributions are equal at $p_{\rm t} \simeq 20$ GeV, and the relative contribution of direct processes increases with increasing $p_{\rm t}$. Right: in the isolated case, the direct processes dominate; at $p_{\rm t} \simeq 20$ GeV, they represent about 75% of the cross section, and that percentage increases with increasing $p_{\rm t}$.

5. Conclusion

Using JetPhox allows us to compute the DPE prompt photon production cross sections with, for the first time, next-to-leading order hard matrix elements. Our main result is that the NLO cross sections are larger than the LO ones, by about 20% in the inclusive case and 50% in the isolated case. NLO corrections are, therefore, crucial in such processes at the 13 TeV LHC. In addition, we observed that the isolation criteria is necessary in order to suppress the contribution of fragmentation photons, radiated by high-$p_{\rm t}$ partons during their fragmentation, and to access in a clean way the direct processes of photon production.

Finally, we have analyzed different possible scenarios to be tested by the LHC experiments ATLAS-AFP and TOTEM–CMS, and we expect that future data on DPE prompt photon production will provide a quantitative way to test the validity of resolved Pomeron model, the factorization of diffractive pdfs into a Pomeron and a Pomeron pdfs, as well as to extract the gap survival probability and understand its behavior with increasing energy. We also hope that $pp \to pp\gamma X$ measurements at 13 TeV will allow to constraint the quark and gluon structure of the Pomeron, as $pp \to \gamma X$ measurements have helped constrain regular parton distribution functions [21, 22].

We thank Jean-Philippe Guillet, Christophe Royon and Maria Ubiali for useful discussions and comments. A.K.K. thanks Victor Gonçalves for useful discussions during the Symposium (ISVHECRI 2014) realized at CERN and also the CAPES-Brazil agency for financial support.

REFERENCES

[1] M. Derrick *et al.* [ZEUS Collaboration], *Phys. Lett. B* **315**, 481 (1993).

[2] T. Ahmed *et al.* [H1 Collaboration], *Nucl. Phys. B* **429**, 477 (1994).

[3] S. Abachi *et al.* [D0 Collaboration], *Phys. Rev. Lett.* **72**, 2332 (1994).

[4] F. Abe *et al.* [CDF Collaboration], *Phys. Rev. Lett.* **74**, 855 (1995).

[5] S. Chekanov *et al.* [ZEUS Collaboration], *Nucl. Phys. B* **816**, 1 (2009).

[6] F.D. Aaron *et al.* [H1 Collaboration], *Eur. Phys. J. C* **72**, 2074 (2012).

[7] F.D. Aaron *et al.* [H1 and ZEUS collaborations], *Eur. Phys. J. C* **72**, 2175 (2012).

[8] J.C. Collins, *Phys. Rev. D* **57**, 3051 (1998) [*Erratum ibid.* **61**, 019902 (2000)].

[9] G. Ingelman, P.E. Schlein, *Phys. Lett. B* **152**, 256 (1985).

[10] A. Aktas *et al.* [H1 Collaboration], *Eur. Phys. J. C* **48**, 715 (2006).

[11] T. Affolder *et al.* [CDF Collaboration], *Phys. Rev. Lett.* **84**, 5043 (2000).

[12] G. Altarelli, G. Parisi, *Nucl. Phys. B* **126**, 298 (1977); V.N. Gribov, L.N. Lipatov, *Sov. J. Nucl. Phys.* **15**, 438 (1972); **15**, 675 (1972); Y.L. Dokshitzer, *Sov. Phys. JETP* **46**, 641 (1977).

[13] C. Marquet, C. Royon, M. Saimpert, D. Werder, *Phys. Rev. D* **88**, 074029 (2013).

[14] M. Boonekamp *et al.*, `arXiv:1102.2531 [hep-ph]`.

[15] C. Brenner Mariotto, V.P. Goncalves, *Phys. Rev. D* **88**, 074023 (2013).

[16] S. Catani, M. Fontannaz, J.P. Guillet, E. Pilon, *J. High Energy Phys.* **0205**, 028 (2002); P. Aurenche *et al.*, *Phys. Rev. D* **73**, 094007 (2006).

[17] J.F. Owens, *Rev. Mod. Phys.* **59**, 465 (1987).

[18] ATLAS Collaboration, Letter of Intent for the Phase-I Upgrade of the ATLAS Experiment, CERN-LHCC-2011-012.

[19] M. Trzebiński, *Proc. SPIE Int. Soc. Opt. Eng.* **9290**, 929026 (2014).

[20] M.R. Whalley, D. Bourilkov, R.C. Group, `arXiv:hep-ph/0508110`.

[21] R. Ichou, D. d'Enterria, *Phys. Rev. D* **82**, 014015 (2010).

[22] D. d'Enterria, J. Rojo, *Nucl. Phys. B* **860**, 311 (2012).